Surface pinning in ferromagnetic films with perpendicular anisotropy

E. Burgos
Departamento de Física, Facultad de Ciencias, Universidad de Chile, Chile

E. Sallica Leva, J. Gómez, F. Martínez Tabares, and M. Vásquez Mansilla
Centro Atómico Bariloche (CNEA), 8400 Bariloche, Río Negro, Argentina

A. Butera*
Centro Atómico Bariloche (CNEA) and Instituto Balseiro (U. N. Cuyo), 8400 Bariloche, Río Negro, Argentina
(Received 30 November 2010; revised manuscript received 30 March 2011; published 6 May 2011)

We have studied the ferromagnetic resonance response in a series of atomically disordered FePt thin films as a function of film thickness (9–200 nm) and excitation frequency (9.5 and 24 GHz). These films are characterized by a perpendicular anisotropy that promotes a stripelike magnetic domain structure above a critical thickness $d_{cr} \sim 30$ nm. All films display a resonant absorption due to the uniform precession of the magnetization vector. The analysis of the linewidth as a function of film thickness shows that the line broadens considerably above d_{cr}. In the thinner films ($d < 28$ nm) we have only observed the absorption related to the uniform precession mode, but thicker films, in which a stripe domain pattern is observed at zero field in static magnetic measurements, show an additional resonance line when the magnetic field is applied at, or very close to, the film plane normal. This line appears at fields below the main resonance and is observed at both X and K bands with approximately the same field separation from the uniform mode. We have also found that the line separation between the two resonances varies with the film thickness, indicating that the appearance of an additional resonance is related to confinement effects, but does not follow the quadratic law expected for infinite surface pinning. The ferromagnetic resonance results have been interpreted within a model of standing spin waves with finite surface pinning. From the angular variation of the pinning parameter close to the film normal we have found that the surface anisotropy is perpendicular to the film plane and increases with film thickness. The origin of the surface anisotropy seems to be related to a substrate-induced strain produced in the fabrication process and to a surface layer with a reduced magnetization. Annealing the samples at relatively low temperatures produces important changes in the resonance spectra. The overall observed behavior suggests that even though the resonance experiments are made at fields large enough to be in a magnetically saturated state, the formation of a stripe structure and the changes observed in the ferromagnetic resonance spectra above d_{cr} are not completely uncorrelated phenomena.

DOI: 10.1103/PhysRevB.83.174417 PACS number(s): 75.70.Ak, 76.50.+g, 75.30.Gw, 75.50.Bb

I. INTRODUCTION

Fe and Co alloys with Pt or Pd have been widely investigated in the past years due to their very large magnetocrystalline anisotropy and the high coercivity that can reach values of several kOe.[1–5] These properties make this system a candidate for ultrahigh density magnetic recording media, and considerable effort has been devoted to study FePt and the other alloys in the form of thin films and nanoparticles.[1,6–11] When this alloy is fabricated in the form of a thin film using sputtering techniques, it generally grows in a disordered fcc phase called A_1 that shows soft magnetic properties[6–8] because the atomic order that is responsible for the hard magnetic behavior cannot be achieved. Even though the soft magnetic phase has limited technological interest (at least as a media for magnetic recording) it has a very rich magnetic behavior. The films show an effective anisotropy perpendicular to the film plane,[8] which is due to the combined effect of magnetocrystalline anisotropy (samples grow with a [111] texture perpendicular to the film plane) and magnetoelastic energy (as-deposited films form under in-plane compressive stress which induces a perpendicular easy axis). The energy associated to this perpendicular anisotropy is smaller than the shape demagnetizing energy, causing the quality factor Q to be less than one ($Q = K_\perp/2\pi M_s^2 < 1$, where $K_\perp$ is the perpendicular anisotropy constant and M_s is the saturation magnetization). This in general implies that the magnetization of the sample should stay in the film plane. However, for thicker films that have a critical value d_{cr}, it is energetically favorable to form domains with a stripe structure in which the magnetization stays essentially in the film plane, but a relatively small perpendicular component points alternatively in the up and down directions. For films with quality factors $Q \sim 0.3$ the critical thickness is in the range 20–40 nm.[8,12,13] The dynamic properties of FePd and FePt films using ferromagnetic resonance (FMR) techniques have been reported by Ben Youssef *et al.*[14] and Martins *et al.*,[15] respectively. In the case of FePd, a 50-nm sample was grown by molecular beam epitaxy (MBE), alternating single atomic layers of Fe and Pd. In spite of the fabrication process, the film showed almost complete atomic disorder in long-range scales with a perpendicular anisotropy $K_\perp \sim 2 \times 10^6$ erg/cm^3 and a quality factor $Q \sim 0.4$. FMR experiments at fields and frequencies large enough to be in a magnetic saturated state showed a perpendicular resonance spectrum with a uniform precession mode (spin wave number $k = 0$) and three additional absorptions that were associated to standing spin wave (SSW) modes (spin wave number $k \neq 0$). These lines

were almost equally spaced by a field of ∼400 Oe, contrary to the expected Kittel's[16] quadratic law on mode number. In the case of FePt films the samples were fabricated by sputtering and had a crystalline texture that was dependent on the use (or not) of a Pt buffer layer. SSWs were observed in both cases (although the number of lines was smaller in the films with a Pt underlayer), and in these samples a quadratic behavior on mode number was found. However, the separation between modes was larger for thicker films, at variance with the predictions of most SSW models.[16,17] To explain these results, the exchange stiffness constant, which was deduced from the field separation between modes, was assumed to vary between $A = 3.9 \times 10^{-8}$ erg/cm and $A = 4.4 \times 10^{-7}$ erg/cm in the two samples. These values are much smaller than that reported from static magnetization measurements by Okamoto *et al.*[1] ($A \sim 1 \times 10^{-6}$ erg/cm), where it was experimentally shown that A is almost independent of the degree of atomic order, so that no significant differences in the value of A are expected if the same alloy is deposited on different substrates or fabricated under different conditions. The above-mentioned FMR results point out the need of further research in the system of disordered FePt alloys to better understand the complex magnetic behavior. Our group has previously reported the observation of additional resonance lines in a very limited set of FePt films that were assigned to SSWs.[6] We are presenting in this work FMR studies in an extended set of thin films with thicknesses in the range 9–200 nm. The dynamic response of the samples has been measured at two different frequencies and the angular behavior of the SSW spectra close to the film normal was carefully analyzed. Results, modeling, and conclusions are presented in the following sections.

II. EXPERIMENTAL DETAILS

The films used in this study are the same samples that we have used in Ref. 8. In short, as-made disordered FePt films have been fabricated by dc magnetron sputtering on naturally oxidized Si (100) substrates. The samples were deposited from an FePt alloy target with a nominal atomic composition of 50/50. The chamber was pumped down to a base pressure of 10^{-7} Torr and the films were sputtered using 2 mTorr of Ar pressure, a power of 20 W, and a target-substrate distance of 5 cm. With these parameters we obtained a sputtering rate of 0.15 nm/s. Nine different films were sputtered with thicknesses of 9, 19, 28, 35, 42, 49, 56, 94, and 200 nm. No capping layer was used because the films were found to be relatively resistant to oxidation. This was confirmed by measuring the same value of saturation magnetization after several months. X-ray diffraction data indicate that as-made samples tend to grow with a high [111] texture normal to the film plane and that they are under an in-plane compressive stress. These two effects tend to produce an effective perpendicular anisotropy $K_\perp = 1.5(4) \times 10^6$ erg/cm^3. From electron dispersive x-ray spectroscopy (EDX) analysis it was found that the Fe/Pt atomic ratio of both the target and the films was ∼45/55. The average grain size estimated from transmission electron microscopy (TEM) micrographs is $\langle D \rangle \sim 4$ nm. Note that this value is smaller that the so-called exchange length $L = \sqrt{A/K_\perp}$, which for films with atomic disorder is $L \gtrsim 7$ nm. For this reason the magnetic response of individual grains is coupled by the exchange interaction and a single, relatively narrow, resonance line is then expected for the uniform resonance mode.

FMR spectra have been acquired at room temperature with a commercial Bruker ESP 300 spectrometer at frequencies of 9.5 GHz (X band) and 24.1 GHz (K band). The samples were placed at the center of a resonant cavity where the derivative of the absorbed power was measured using a standard field modulation and lock-in detection technique with amplitudes in the range 5–20 Oe. The film plane was in all cases parallel to the excitation microwave field. Angular variations with respect to the external dc field were made around the film normal in an angular range of ±5° with a specially designed goniometer that has a resolution of better than 0.1° (only in the X-band setup). The maximum available dc field was 19 kOe.

III. EXPERIMENTAL RESULTS AND MODEL

In Ref. 6 we have reported the resonance spectra for the cases in which the external field was applied either parallel or perpendicular to the film plane. We have found that a single resonance line was always observed for the in-plane configuration while one or two absorptions could be observed when the field H was applied normal to the film plane, depending on the film thickness. Due to the very limited number of samples available it was not possible in that study to correlate precisely the appearance of new absorption lines with the variation of film thickness. In this work we have paid special attention to the thickness range close to d_{cr} in order to check for variations in the characteristics of the absorption line as the film thickness is changed. As is well known, the resonance field in a ferromagnetic film depends on the excitation frequency and the film orientation. For the X band we have obtained the following average values for the resonance field of the most intense resonance in the two geometries: $\langle H_{r||} \rangle \sim 1050$ Oe and $\langle H_{r\perp} \rangle \sim 12\,100$ Oe, while for K band $\langle H_{r||} \rangle \sim 5050$ Oe and $\langle H_{r\perp} \rangle \sim 17\,100$ Oe. Evidence that films thinner or thicker than d_{cr} show a different dynamic response, even at fields larger than those needed to saturate the magnetization of the samples,[18] is presented in Fig. 1. In this figure we show the linewidth ΔH_r of the uniform mode as a function of film thickness when the external field is applied in the film plane or perpendicular to it for X- and K-band frequencies. It can be observed that the perpendicular linewidth is almost constant, except for a very small increase close to d_{cr} at the K band. On the contrary, the parallel linewidth increases considerably above d_{cr}. In the figure we have marked with dashed lines the average value of $\Delta H_{r||}$ in the two regions and the estimated change in $\Delta H_{r||}$ is 80 ± 20 Oe for the X band and 100 ± 20 Oe for the K band. The possible origin of the increase of the parallel linewidth was discussed in Ref. 7 and is closely related to the presence of rotatable anisotropy[8] in films thicker than d_{cr}. Films with an in-plane domain structure ($d < d_{cr}$) show in general a small in-plane easy axis of anisotropy which is independent of the magnetic history of the sample. On the other hand, films with a stripe magnetic structure tend to have the stripes aligned parallel to the direction where a strong enough field was previously applied. In this case the in-plane easy axis is more randomly distributed and the misalignment contributes to the

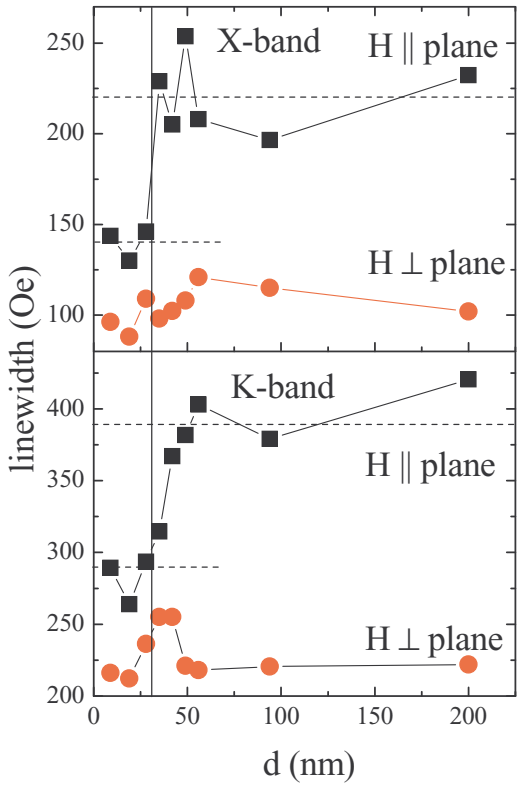

FIG. 1. (Color online) Linewidth as a function of film thickness for the X and K bands. At both frequencies a sharp increase is observed at the critical thickness (represented by a thin vertical line) when the field is applied parallel to the film plane. Error bars are of the order of the symbol size.

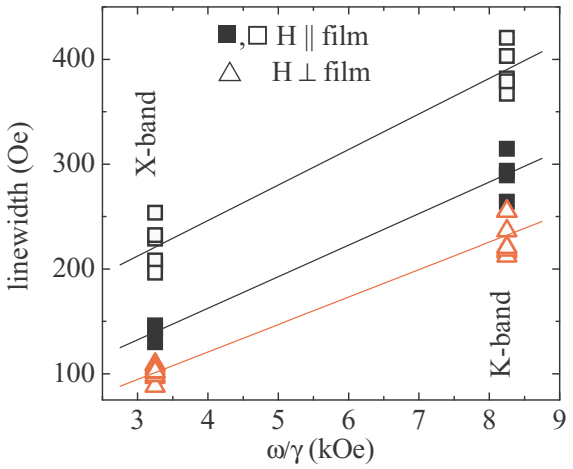

FIG. 2. (Color online) Linewidth as a function of frequency for X and K bands. Closed and open squares correspond to $d < d_{cr}$ and $d > d_{cr}$, respectively, in the case of parallel resonance. Triangles have been used for the case of perpendicular resonance. Continuous lines are linear fits with a slope proportional to the intrinsic damping coefficient, and an ordinate that gives the extrinsic contribution to the linewidth.

inhomogeneous broadening of the absorption. In general, the line broadening can be described by a term that depends linearly on frequency, and a nonlinear contribution arising from the distribution of grain sizes, shapes, anisotropies, and other scattering mechanisms.[19–23] In the case of a distribution of anisotropy easy axes the nonlinear contribution to ΔH_r can be approximated by a constant factor, independent of frequency, that is proportional to the in-plane effective anisotropy,[7] The broadening in the data measured at the K band (100 ± 20 Oe) is somewhat larger than the values obtained at the X band (80 ± 20 Oe), but both agree within the experimental error. In Fig. 2 we show the linewidth as a function of frequency for parallel an perpendicular geometries. In the case of parallel resonance we have distinguished the data with closed (for $d < d_{cr}$) and open (for $d > d_{cr}$) symbols according to the film thickness. In the perpendicular case no clear features can be distinguished at d_{cr}. The linewidth was fit with a linear law ($\Delta H_r = \frac{2}{\sqrt{3}}\alpha\omega/\gamma + \Delta H_{r0}$) which gives almost the same value of the damping coefficient in both geometries and in the two regions of $\Delta H_{r||}$, $\alpha = 0.027 \pm 0.003$, confirming that the intrinsic damping mechanism is independent of film thickness and orientation, as expected. This value of α is larger than the reported coefficient for pure Fe ($\alpha = 0.002$–0.006),[24] but in the range of what can be found in Fe alloys.[25] The value of the frequency-independent term depends on the orientation and also on film thickness in the case of $\Delta H_{r||}$. This term is considerable higher above d_{cr} ($\Delta H_{r0||} = 111 \pm 16$ Oe) than in the region $d < d_{cr}$, $\Delta H_{r0||} = 42 \pm 17$ Oe, again consistent with a larger distribution of anisotropy axes in films thicker than d_{cr}. The extrinsic contribution in the case of perpendicular geometry, $\Delta H_{r0\perp} = 16 \pm 8$ Oe, is lower than the values in the parallel configuration, probably due to the negligible effect of the two-magnon-scattering mechanism in this orientation.

The most distinctive feature that is observed in films thicker than d_{cr} is the appearance of an additional absorption line when the external field is applied within $\pm 5^\circ$ of the film normal. In all samples this line is detected at fields lower than the uniform resonance, and the field separation between both lines depends strongly on the film thickness. In Fig. 3 we show the X-band spectra measured with H perpendicular to the film plane. Similar spectra is observed at higher frequencies (K band) with the only difference that we have not been able to detect the extra absorption in the sample with $d = 28$ nm. This could be due to the very small intensity of the additional absorption, which is less than 3% of the intensity of the uniform mode in X-band measurements. The $d = 200$ nm film has not been included in the following analysis because for this sample the microwave skin depth is of the same order as the film thickness[26] and then the microwave field is not uniform inside the sample. In this situation it is possible to excite additional modes which complicate the interpretation of the resonance spectra. In fact, an additional absorption structure is observed in the experimental spectra of this film taken at both X- and K-band frequencies. For this same reason the K-band spectrum of the 94-nm film must be interpreted with extra care.

The field separation in the perpendicular geometry between the uniform resonance mode ($H_{r0\perp}$) and the additional mode ($H_{r1\perp}$) has been plotted as a function of film thickness in Fig. 4 in a log-log scale. It can be seen that the separation between modes follows a power law and is practically independent of frequency, with the exception of the 94-nm film in the K band which, as previously mentioned, has a skin depth lower than the film thickness at this frequency.

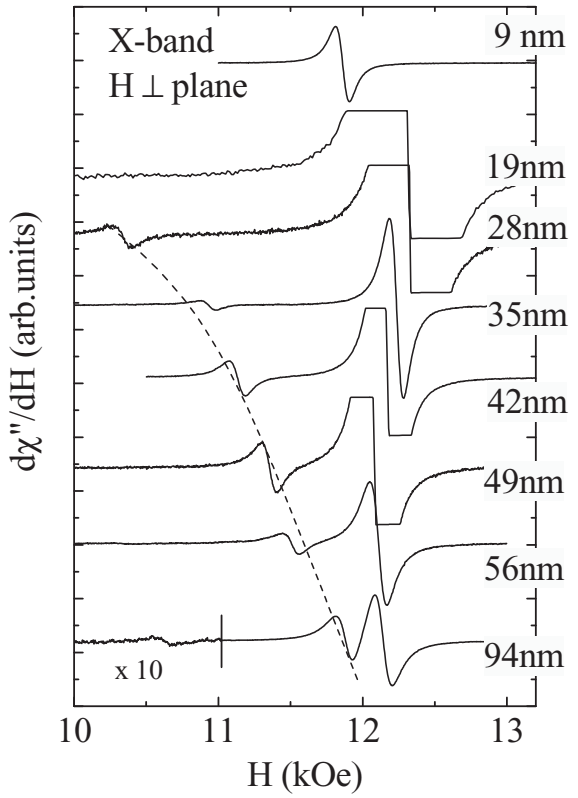

FIG. 3. *X*-band spectra for different thicknesses acquired with H perpendicular to the film plane. In some cases the uniform mode is saturated to allow for the observance of the additional absorption. The dashed line is a guide to the eye to stress the variation of the resonance field with film thickness. In the sample with $d = 94$ nm we have multiplied by a factor of 10 the low-field part of the spectrum.

The general theory and phenomenology of ferromagnetic resonance spectroscopy can be found in the book of Gurevich and Melkov.[27] In the present case we will start our discussion using the dispersion relation that permits to obtain the resonance fields in the case of nonuniform excitations:[28,29]

$$\left(\frac{\omega}{\gamma}\right)^2 = \left[H_{rn}\cos(\phi-\phi_H) - H_{\text{eff}}\cos^2\phi + \frac{2A}{M_s}k_n^2\right] \times \left[H_{rn}\cos(\phi-\phi_H) - H_{\text{eff}}\cos 2\phi + \frac{2A}{M_s}k_n^2\right], \tag{1}$$

where ω is the microwave angular frequency, $\gamma = g\mu_B/\hbar$ is the gyromagnetic ratio, H_{rn} is the resonance field for mode n, H_{eff} is the effective anisotropy field, k_n is the wave number for mode n, and ϕ and ϕ_H are the angles that the magnetization and the external field form with the film normal. Note that for a given mode two values of the wave vector k_n can be obtained from Eq. (1) if the other parameters are known. One of the k_n values can be real or complex and the other is purely imaginary. The angle ϕ is different for each resonance mode and can be estimated numerically from the equilibrium equation for the static magnetization vector:

$$2H_{rn}\sin(\phi-\phi_H) - H_{\text{eff}}\sin 2\phi = 0. \tag{2}$$

The experimental setup corresponds to the film placed in the yz plane, the external field rotating in the xy plane, and the microwave field applied in the z axis. In Kittel's model it is assumed that spin waves have nodes at the surfaces of the film and the wave number is then proportional to the film thickness, $k_n = n\pi/d$. Assigning $n = 0$ and $n = 1$ to the uniform and the first excited modes,[30] for perpendicular resonance ($\phi = 0$) it is then possible to deduce an expression for the thickness dependence of the field difference between the two modes from Eq. (1),

$$\delta H_\perp = H_{r0\perp} - H_{r1\perp} = \frac{2A}{M_s}\left(\frac{\pi}{d}\right)^2. \tag{3}$$

This equation has been plotted in Fig. 4 for $A = 0.95 \times 10^{-6}$ erg/cm and $M_s = 866$ emu/cm^3, the estimated values for our FePt films.[1,8] From the experimental data it is clear that the thickness dependence of $\delta H_\perp$ does not obey a $1/d^2$ law as expected in the case of perfect pinning, although a power-law behavior is still observed with a slope of $\sim$1.7. Note that if spins are not infinitely pinned at the surface, a power of lower than 2 can be found. For example, in the case of a quadratic decrease with distance of M_s close to the surface, a linear behavior is predicted (the Portis model, see Ref. 17). The situation of finite surface pinning has been treated in great detail by many authors[31–35] in the case of uniform magnetization in the bulk of the film, when the so-called surface inhomogeneity model is applicable. This model assumes that spins at the surface experience a different local field than bulk spins, which is determined by the surface free energy F_s and the normal derivative of the magnetization vector $\partial_n \mathbf{M}$. The Rado-Weertman[36] boundary conditions at the

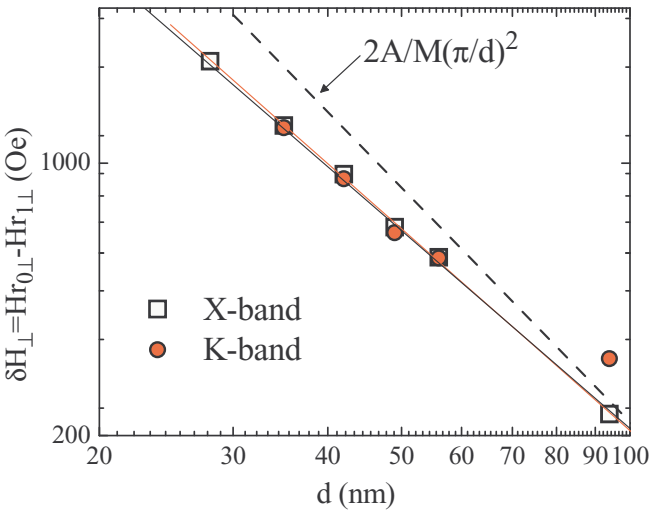

FIG. 4. (Color online) Field separation between the uniform and the first excited mode in the perpendicular geometry ($H \perp$ film plane). Data correspond to measurements at 9.5 GHz (*X* band) and 24.1 GHz (*K* band). Continuous lines are linear best fits to the experimental values. The 94-nm film was not considered in the case of the *K* band for the reasons discussed in the text. The dashed line indicates the expected slope for infinite surface pinning.

surface are used to relate these two quantities with the wave vector k:

$$\begin{aligned} \partial_n m_\theta + p m_\theta + r m_\phi &= 0, \\ \partial_n m_\phi + q m_\phi + r m_\theta &= 0, \end{aligned} \tag{4}$$

with

$$\begin{aligned} p &= \frac{1}{2A}\frac{\partial^2 F_s}{\partial\theta^2} - \frac{\partial_n M_s}{M_s}, \\ q &= \frac{1}{2A}\left[\frac{\cos\theta}{\sin\theta}\frac{\partial F_s}{\partial\theta} + \frac{1}{\sin^2\theta}\frac{\partial^2 F_s}{\partial\phi^2}\right] - \frac{\partial_n M_s}{M_s}, \\ r &= \frac{1}{2A}\left[-\frac{\cos\theta}{\sin^2\theta}\frac{\partial F_s}{\partial\phi} + \frac{1}{\sin^2\theta}\frac{\partial^2 F_s}{\partial\theta\,\partial\phi}\right]. \end{aligned} \tag{5}$$

In the above equations m_θ and m_ϕ are the components of the oscillating magnetization in the directions of the polar and azimuthal angles of the magnetization vector, $\hat{\theta}$ and $\hat{\phi}$. The parameters p and q are known as the pinning parameters. In the single wave-vector approximation[33] the purely imaginary solution for k_n is not considered in Eq. (1) and the magnetization components are given by

$$\begin{aligned} m_\theta &= A_0 \sin kx + A_1 \cos kx, \\ m_\phi &= A_2 \sin kx + A_3 \cos kx. \end{aligned} \tag{6}$$

The simplest form for the surface anisotropy is to assume an easy anisotropy axis, $F_s = K_s \cos^2\phi \sin^2\theta$. If $K_s < 0$ the easy axis is normal to the film plane (parallel to $\hat{x}$), and for $K_s > 0$ the surface energy is minimized if M is within the film plane (the plane yz is an easy anisotropy plane). Considering this form of F_s and setting $\theta = \theta_{\rm eq} = \pi/2$ we can obtain

$$\begin{aligned} p &= -\frac{K_s}{A}\cos^2\phi - \frac{\partial_n M_s}{M_s}, \\ q &= -\frac{K_s}{A}\cos 2\phi - \frac{\partial_n M_s}{M_s}, \\ r &= 0. \end{aligned} \tag{7}$$

As can be seen from Eq. (7) for $\phi = 0$ the values of p and q are coincident ($p = q = -\frac{K_s}{A} - \frac{\partial_n M_s}{M_s}$). Close to the film normal the angles ϕ_H and ϕ are small, and $\cos^2\phi$ can be approximated by $\cos 2\phi$. In this case $p \simeq q$ and it is enough to evaluate one of Eqs. (4) at both surfaces of the film ($p = p_d$ for $x = d$ and $p = p_0$ for $x = 0$) to arrive at the following expressions:

$$\begin{aligned} A_0(k\cos kd + p_d \sin kd) + A_1(-k\sin kd + p_d \cos kd) &= 0, \\ -A_0 k + p_0 A_1 &= 0. \end{aligned} \tag{8}$$

Setting the determinant of Eq. (8) equal to zero gives the relationship between the wave vector and the pinning parameters,

$$\tan kd = \frac{k(p_0 + p_d)}{2k^2 - p_0 p_d}, \tag{9}$$

which, assuming symmetrical surfaces ($p_0 = p_d = p$), can be simplified to

$$\tan kd = \frac{2kp}{2k^2 - p^2}. \tag{10}$$

From the above equation it is possible to obtain a closed expression for the pinning parameter p if the wave vector k is known. The value of k can be calculated as a function of the angle ϕ_H of the external applied field (and also the angle ϕ_1 of the magnetization) from the resonance field of the additional line using Eq. (1). We have used the values of A and M_s already mentioned, assumed $g = 2.09$ for FePt,[6] and calculated ϕ_1 from Eq. (2) (note that the static magnetization angle is slightly different in this case because the resonance occurs at a field lower than that of the uniform mode). The effective anisotropy field is estimated from the resonance of the uniform mode in the perpendicular configuration (see Table I). Once the pinning parameter is known, it is possible to calculate the value of k_n for the higher-order excited modes solving Eq. (10) numerically. In Ref. 33 the author gives an expression to estimate the relative intensity of the excited modes:

$$I_n = \frac{2\sin^2(k_n d/2)/(k_n d/2)^2}{1 + \sin(k_n d)/(k_n d)}. \tag{11}$$

In the case of symmetric surfaces and perfect pinning the intensity of even-order modes is predicted to be zero, while that of odd modes decays approximately as $1/(k_n d)^2$. From Eq. (1) we estimated the field at which the excited modes should be observed for different values of d. For $d = 28$ and 35 nm the resonance field for the modes with $n \geqslant 3$ is expected to occur at negative fields, and then these absorptions are not observable. In the films with $d \geqslant 42$ nm, the mode with $n = 3$ should be observed, but we were not able to detected any additional line, probably due to the $1/(k_n d)^2$ dependence of the intensity of higher-order modes. In this regard there are reports[37] that the linewidth of the excited modes tends to increase proportionally to k_n^2 when the sample is magnetically inhomogeneous or if there are variations in the film thickness. This effect also reduces the amplitude of the absorption signal and complicates the detection of the excited modes. In the thicker samples (see the bottom curve of Fig. 3 corresponding to the film with $d = 94$ nm) we have been able to detect an absorption of very low intensity (almost 100 times smaller than I_1) that is close to the position where the $n = 2$ mode is expected. The extremely low intensity of this absorption corresponding to an even mode supports our previous assumption that the samples can be treated as nearly symmetric films. To simplify the analysis of the experimental data, modes with $n \geqslant 2$ will not be considered in the rest of this work.

In all films where an additional line is observed we have measured at the X band the angular variation of both absorptions close to the film normal. In Fig. 5 we present the field separation between both modes as a function of the angle

TABLE I. Effective anisotropy field as a function of film thickness estimated from the measurements at the X band.

d (nm)	$H_{\rm eff}$ (Oe)
28	9000
35	8860
42	8970
49	8780
56	8800
94	8720

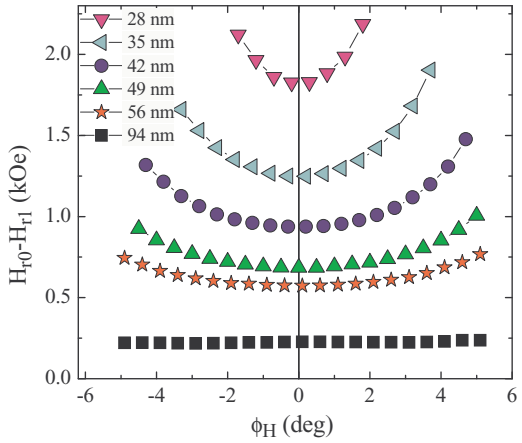

FIG. 5. (Color online) Field separation between the resonance of the uniform and the first excited modes as a function of the angle ϕ_H that the external field forms with the film normal. Data correspond to measurements at 9.5 GHz.

ϕ_H. In the case of thicker films the SSW mode is detected in an angular range of $\pm 5^\circ$ from the film normal, while for thinner films it can only be observed in a range of $\pm 2^\circ$. In all samples the separation between modes $(H_{r0} - H_{r1})$ tends to be larger as the external field is moved away from the film normal. This difference is relatively constant for $d = 94$ nm and increases more rapidly as the film thickness is decreased.

This angular variation, together with Eqs. (1) and (2), was used to estimate the value of the wave vector k as a function of angle, which in turn can be used to calculate the angular dependence of the pinning parameter p from Eq. (10). As can be seen in Fig. 6, in the small-angle approximation the pinning parameter is a linear function of $\cos 2\phi_1$. The linear behavior has been observed to hold in all films for $\cos 2\phi_1 \gtrsim 0.9$, which corresponds to $\phi_H \lesssim 2^\circ$. For larger angles the calculated angular dependence of p starts to depart from a linear law. From the fit of the angular variation of p in the linear region it is possible to estimate the thickness dependence of the surface anisotropy and the variation of the magnetization in the surface layer. The dependence of K_s and $\partial_n M_s$ as a function of d is plotted in Fig. 7. We have found a negative value of K_s in all films, indicating that the surface anisotropy favors an easy axis perpendicular to the film plane. The absolute values are in the range $K_s = 0.06$–0.45 erg/cm^2. As far as we know there are no reported values of the surface anisotropy constant in FePt films, but they can be compared with the values reported[38] for pure Fe films obtained using dc magnetization techniques ($K_s = 0.14$–1.45 erg/cm^2 and in all cases favors an easy axis perpendicular to the film plane), or with the values obtained using FMR techniques in ferromagnetic materials such as iron[39] ($K_s = 0.5$–1 erg/cm^2), permalloy[29] ($K_s = 0.1$–0.5 erg/cm^2), FeBSi (Ref. 40) ($K_s = 0.13$ erg/cm^2), GdCoMo (Ref. 41) ($K_s = 0.4$–0.85 erg/cm^2), and Co-SiO_2 granular materials[35] ($K_s = 2$–4 erg/cm^2). We have also observed a tendency of the surface anisotropy to increase as the film thickness increases. This behavior has been reported by many authors in different films both in the ultrathin limit (Heinrich *et al.*[39] reported a twofold increase in K_s when d changes from 0.4 to 4 nm) or in the thicker limit (K_s changes from 0.2 to 0.5 erg/cm^2 when d passes from 80 to 270 nm in permalloy films[29] and increases by a factor 1.5 in GdCoMo films[41]).

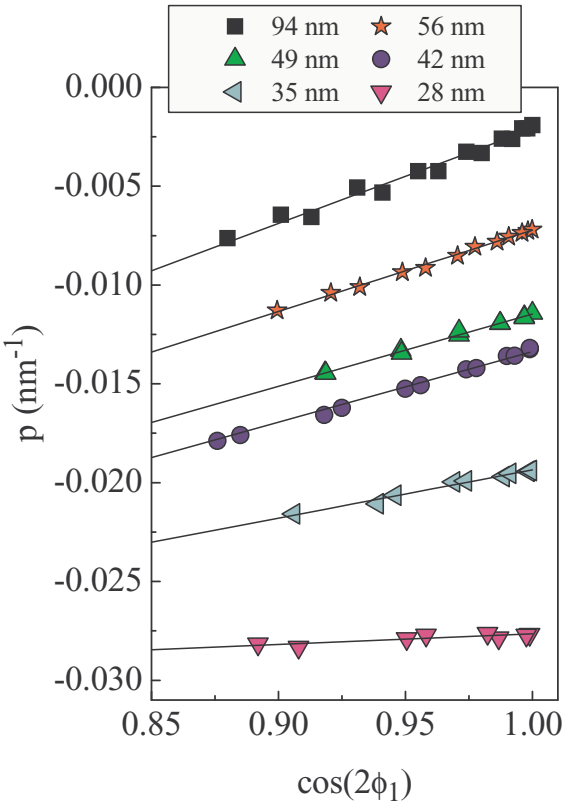

FIG. 6. (Color online) Variation of the pinning parameter p as a function of $\cos 2\phi_1$ for different thicknesses. Continuous lines correspond to linear fits using Eq. (7). Data have been obtained from measurements made at 9.5 GHz.

The parameter $\partial_n M_s$ is also thickness dependent and tends to saturate for $d > 40$ nm to a value $\partial_n M_s \sim 43$ emu/cm^3/nm or $\partial_n M_s / M_s \sim 0.05$ nm^{-1}. There are less reported values[42] of $\partial_n M_s$ than for the surface anisotropy, but in general they are consistent with the data we have found in our FePt films. An increasing value of $\partial_n M_s$ with film thickness was also reported by Maksymowicz *et al.*[41] in GdCoMo films.

A complete description of magnetic surface anisotropy should include a full calculation of the electronic band structure. However, from the phenomenological point of view, it is enough in many cases to take into account a few selected contributions that can explain the observed behavior.[29,41] The effect of a broken symmetry at the film surface is usually explained by Néel's model,[29,43] which relates the surface anisotropy constant to the magnetoelastic (B_1 and B_2), elastic (c_{11}, c_{22}, c_{44}), and magnetostriction (λ_{100}, λ_{111}) constants of the material,

$$K_s^N = \frac{V}{2Na^2}\left(\frac{B_2 - 2B_1}{3}\right) = \frac{a}{8}\left[(c_{11} - c_{22})\,\lambda_{100} - c_{44}\lambda_{111}\right], \tag{12}$$

where V is the molar volume, a the lattice constant, and N the Avogadro number. As mentioned in Ref. 41, Néel's theory works well in the very thin limit, but for films in the range of hundreds of nanometers it is necessary to consider additional

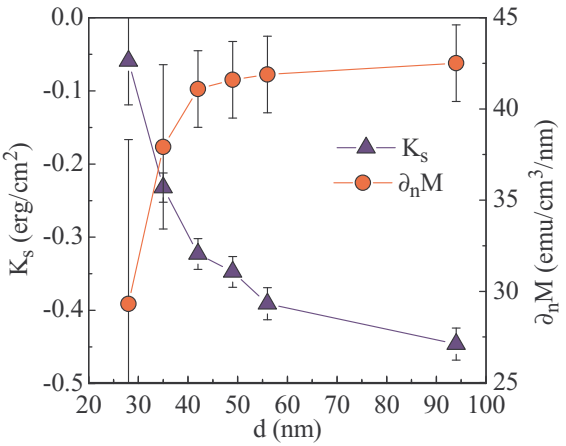

FIG. 7. (Color online) Surface anisotropy and magnetization variation at the surface as a function of film thickness obtained from the linear fits of Fig. 6.

contributions to the surface anisotropy. If the surface is not protected, or if there is interdiffusion with the capping layer, it is possible that a thin layer of thickness Δd close to the surface has a magnetization different than the bulk value by an amount ΔM. In the case of FePt there are reports of selective Fe oxidation when the film is exposed to air.[44] However, we have repeated measurements of the same samples (that were stored in air) after several months and did not find any significant reduction in the saturation magnetization so that the oxidation, if present, is limited to a thin surface layer. If a region of thickness Δd has magnetization $M_s - \Delta M$, the magnetic energy of this region can be written as[45] $E = 2\pi(M_s - \Delta M)^2 \sim 2\pi M_s^2 - 4\pi M_s \Delta M$. The additional term in the energy can be interpreted as an extra term for the surface anisotropy,

$$K_s^{\Delta d} = 4\pi M_s \Delta M \Delta d. \tag{13}$$

In a first approximation that assumes independent contributions of both terms, the total surface anisotropy can be expressed as $K_s = K_s^N + K_s^{\Delta d}$. The variation in the magnetization close to the film surface can be related[41] with the derivative of Eq. (7), $\Delta M/\Delta d = -\partial_n M_s$, so that it is possible to estimate the thickness of the surface layer from the parameters obtained from the FMR measurements,

$$\Delta d = \sqrt{\left|\left(K_s - K_s^N\right)/(4\pi M_s \partial_n M_s)\right|}. \tag{14}$$

In order to check the validity of the interpretation of the experimental data, we have made an order of magnitude estimation of K_s^N using the measured bulk values for A_1 alloys and Eq. (12). For the magnetostriction constant we have used the value reported by Aboaf *et al.*[46] ($\langle\lambda\rangle = 7 \times 10^{-5}$) in polycrystalline samples and assumed $\lambda_{100} = \lambda_{111}$. Values for the elastic constants in FePt have not been reported as far as we know, so we have used data available for FePd crystals[47] ($c_{11} - c_{22} = 0.54 \times 10^{12}$ dyn/cm^2 and $c_{44} = 0.832 \times 10^{12}$ dyn/cm^2). The estimation gives $\left|K_s^N\right| \sim 0.1$ erg/cm^2, which is in the same range than the value calculated from the FMR measurements in the 28-nm film and supports the model used to obtain the surface anisotropy. The parameter K_s^N is in general assumed to be independent of film thickness, but there are reports showing that stress effects can produce a variation of the magnetoelastic (and hence the magnetostriction) constants. For example, Sander *et al.*[48] have found that in Fe films the effective magnetoelastic constant B_1 departs considerably from its bulk value when the film thickness is varied in the range 1–70 nm. They even observed a change in sign at a thickness of 20 nm. This behavior was due to a thickness-dependent strain which is reduced from $\varepsilon \sim 0.006$ to $\varepsilon \sim 0.004$ in the range 20–70 nm. In our films we only have an estimation of the strain[8] for the film with $d =$ 94 nm, $\varepsilon \sim 0.0067$, so it is possible that part of the observed dependence of K_s in Fig. 7 is due to a substrate-induced stress that depends on film thickness. In this aspect we will later discuss the effects of annealing on the surface anisotropy, however, it is difficult to make a deeper analysis within this model if the thickness dependence of the strain is not known, and for simplicity we have assumed $|K_s^N| \sim 0.06$ erg/cm^2, the value measured in the 28-nm film.

The estimation of the surface layer Δd as a function of d is plotted in Fig. 8, where it can be seen that the values of Δd change from 2.1 to 2.9 nm. We have omitted the data for the sample of 28 nm because it was used for the estimation of K_s^N. Considering that the lattice parameter of the alloy is $a =$ 0.3866 nm and that the film is textured in the [111] direction, the value of Δd varies between 5 and 6.5 monolayers in each of the two film surfaces, implying that the surface magnetic layer is relatively well defined because it only changes by ± 1 atomic monolayer in the thickness range 35–94 nm.

To get a deeper insight into the role that tensions play in the magnetic response of the films, we have studied the effects of a moderate temperature annealing in one sample of 94 nm. In Fig. 9 we show two spectra for this sample measured at room temperature with the field applied perpendicular to the film plane. One spectrum corresponds to the sample in the as-made state (similar to the spectrum shown in Fig. 3) and the other was acquired after the same sample has been heated to 525 K. Two main features are observed in the film that was heat treated: There is a shift of the uniform mode to higher fields by almost 640 Oe and the separation between the two modes is considerably increased. We have assigned the shift of the resonance lines to higher fields to an increase

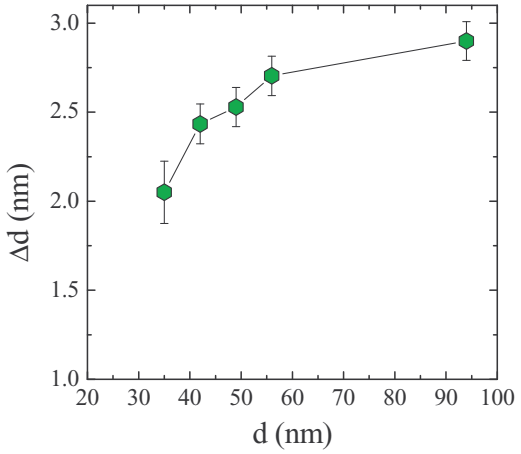

FIG. 8. (Color online) Surface layer thickness as a function of the film thickness obtained from the data of Fig. 7 and Eq. (14).

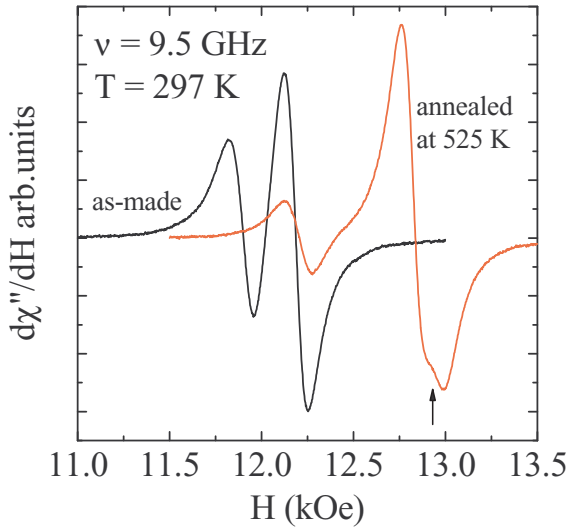

FIG. 9. (Color online) *X*-band FMR spectra for the 94-nm sample with the field applied perpendicular to the film plane measured at room temperature. The left-hand spectrum corresponds to the sample in the as-made state and the right-hand spectrum was acquired after the sample was heated to 525 K inside the cavity. The arrow indicates an absorption of very low intensity occurring at fields larger than the uniform resonance mode.

of the effective anisotropy field, $H_{\rm eff} = 4\pi M_s - 2K_\perp/M_s$. As M_s remains almost unchanged after the heat treatment, the increase in $H_{\rm eff}$ is then related to a reduction in the perpendicular anisotropy. We have already reported in Ref. 8 that the annealing of the films at temperatures as low as 250 °C is enough to reduce the strain and the [111] texture that favor an easy axis perpendicular to the film plane so that a reduction of $K_\perp$ in annealed samples should be expected. If for the as-made film we take $K_\perp = 1.5(4) \times 10^6$ erg/cm^3 and $M_s = 866(25)$ emu/cm^3, the perpendicular anisotropy field is $2K_\perp/M_s \sim 3450$ Oe. In the annealed sample this value should decrease by 640 Oe in order to explain the increase in $H_{\rm eff}$, which means that the perpendicular anisotropy is reduced by ∼20%. The other important change observed in the resonance spectrum is the increase in the separation between the uniform and the first excited modes $\delta H_\perp = H_{r0\perp} - H_{r1\perp}$ from 300 to 625 Oe. As we have already discussed that the separation between modes can be related to the surface anisotropy. The value of $\delta H_\perp$ observed in the annealed film of 94 nm is similar to the value of $\delta H_\perp$ for the 56-nm film, which has a smaller absolute value of the surface anisotropy, as can be seen in Fig. 7. The increase in $\delta H_\perp$ in the heat-treated film then indicates that the release of strain after the annealing procedure changes not only the perpendicular anisotropy but also reduces the absolute value of the surface anisotropy. Apart from these two absorptions there is also an additional mode of very weak intensity occurring at fields higher than the main resonance, which is probably due to a surface mode of the imaginary wave vector, which has not been considered in the present discussion, but is also indicative of a change in the characteristics of the surface. All these features are suggesting that additional studies must be made in order to fully understand the effects of annealing on the magnetic properties of the films.

IV. CONCLUSIONS

We have made a detailed analysis of the dynamic response of the magnetization in as-made FePt thin films, particularly studying the appearance of additional resonance modes above the critical thickness for the formation of magnetic stripe domains. The variation of the separation between the uniform mode and the first excited mode as a function of film thickness and angle can be very well explained with a single value of the exchange stiffness constant, which is generally accepted for thin FePt films. However, it was necessary to take into account that the standing spin waves are not infinitely pinned at the film surfaces, introducing a finite surface anisotropy. We have found that the strain induced in the fabrication process plays an important role in the observed dependence of the surface anisotropy with film thickness. We also observed that the release of tensions through an annealing at low temperatures affects not only the perpendicular anisotropy, but also the surface anisotropy. The surface layer, with a magnetization that is different from the bulk, was estimated to be in the range $\Delta d = 2.1$–2.9 nm, and is weakly dependent on film thickness. Although some correlation was observed, simultaneous measurements of dc magnetization, magnetic force microscopy, and FMR are needed in order to correlate the irreversible changes that occur in annealed samples.

ACKNOWLEDGMENTS

This was supported in part by Conicet under Grant No. PIP 112-200801-00245, ANPCyT under Grant No. PME # 1070, and U.N. Cuyo under Grant No. 06/C235, all from Argentina. Technical support from Julio C. Pérez and Rubén E. Benavides is greatly appreciated.

*butera@cab.cnea.gov.ar; also at Consejo Nacional de Investigaciones Científicas y Técnicas, Argentina.

[1] S. Okamoto, N. Kikuchi, O. Kitakami, T. Miyazaki, Y. Shimada, and K. Fukamichi, Phys. Rev. B **66**, 024413 (2002).

[2] K. R. Coffey, M. A. Parker, and J. K. Howard, IEEE Trans. Magn. **31**, 2737 (1995).

[3] R. A. Ristau, K. Barmak, L. H. Lewis, K. R. Coffey, and J. K. Howard, J. Appl. Phys. **86**, 4527 (1999).

[4] S. Jeong, Y.-H. Hsu, D. E. Laughlin, and M. E. McHenry, IEEE Trans. Magn. **37**, 1299 (2001).

[5] R. F. C. Farrow, D. Weller, R. F. Marks, M. F. Toney, S. Hom, G. R. Harp, and A. Cebollada, Appl. Phys. Lett. **69**, 1166 (1996).

[6]M. Vásquez Mansilla, J. Gómez, and A. Butera, IEEE Trans. Magn. **44**, 2883 (2008).
[7]M. Vásquez Mansilla, J. Gómez, E. Sallica Leva, F. Castillo Gamarra, A. Asenjo Barahona, and A. Butera, J. Magn. Magn. Mater. **321**, 2941 (2009).
[8]E. Sallica Leva, R. C. Valente, F. Martínez Tabares, M. Vásquez Mansilla, S. Roshdestwensky, and A. Butera, Phys. Rev. B **82**, 144410 (2010).
[9]S. Sun, C. B. Murray, D. Weller, L. Folks, and A. Moser, Science **287**, 1989 (2000).
[10]J. M. Vargas, R. D. Zysler, and A. Butera, Appl. Surf. Sci. **254**, 274 (2007).
[11]A. Butera, S. S. Kang, D. E. Nikles, and J. W. Harrell, Physica B **354**, 108 (2004).
[12]M. Hehn, S. Padovani, K. Ounadjela, and J. P. Bucher, Phys. Rev. B **54**, 3428 (1996).
[13]V. Gehanno, Y. Samson, A. Marty, B. Gilles, and A. Chamberod, J. Magn. Magn. Mater. **172**, 26 (1997).
[14]J. Ben Youssef, H. Le Gall, N. Vukadinovic, V. Gehanno, A. Marty, Y. Samson, and B. Gilles, J. Magn. Magn. Mater. **202**, 277 (1999).
[15]A. Martins, S. C. Trippe, A. D. Santos, and F. Pelegrini, J. Magn. Magn. Mater. **308**, 120 (2007).
[16]C. Kittel, Phys. Rev. **110**, 1295 (1958).
[17]A. M. Portis, Appl. Phys. Lett. **2**, 69 (1963).
[18]Due to the formation of a stripe domain structure this assumption is not strictly true for the thicker samples at the *X* band, especially for the 94-nm film which has an in-plane saturation field of ∼1500 Oe. In the case of the *K* band, the in-plane resonance fields are in the range of 5000 Oe, which is well above saturation.
[19]A. Butera, J. N. Zhou, and J. A. Barnard, Phys. Rev. B **60**, 12270 (1999).
[20]A. Butera, J. Gómez, J. L. Weston, and J. A. Barrnard, J. Appl. Phys. **98**, 033901 (2005).
[21]M. J. Hurben and C. J. Patton, J. Appl. Phys. **83**, 4344 (1998).
[22]K. Lenz, H. Wende, W. Kuch, K. Baberschke, K. Nagy, and A. Jánossy, Phys. Rev. B **73**, 144424 (2006).
[23]A. Butera, Eur. Phys. J. B **52**, 297 (2006).
[24]J. Pelzl, R. Meckenstock, D. Spoddig, F. Schreiber, J. Pflaum, and Z. Frait, J. Phys. Condens. Matter **15**, S451 (2003); Z. Celinski and B. Heinrich, J. Appl. Phys. **70**, 5935 (1991); Bijoy K. Kuanr, R. E. Camley, and Z. Celinski, *ibid.* **95**, 6610 (2004).
[25]J.-M. L. Beaujour, A. D. Kent, D. W. Abraham, and J. Z. Sun, J. Appl. Phys. **103**, 07B519 (2008); K. Seemann and H. Leiste, J. Magn. Magn. Mater. **321**, 742 (2009).
[26]The room-temperature skin depth of Fe films is (Ref. 34) ∼40 nm at 10 GHz and 25 nm at 24 GHz. Assuming the same permeability for FePt that has a resistivity eight times larger than Fe (Ref. 46) the estimated skin depth is 112 nm at 10 GHz and 70 nm at 24 GHz.
[27]A. G. Gurevich and G. A. Melkov, *Magnetization Oscillations and Waves* (CRC Press, Boca Raton, FL, 1996).
[28]R. F. Soohoo, Phys. Rev. **131**, 594 (1963).
[29]G. C. Bailey and C. Vittoria, Phys. Rev. B **8**, 3247 (1973).
[30]Strictly speaking, the assignment of $n = 0$ and $n = 1$ to the first two modes is not correct because the $n = 0$ mode can be only excited in the case of uniform magnetization and no surface pinning. If the first mode is $n = 1$, the second can be $n = 2$ or $n = 3$ depending on the symmetry of the pinning. In any case this assignment will produce a shift of the dashed curve in Fig. 4 but not a change in the slope.
[31]H. Puszkarski, Prog. Surf. Sci **9**, 171 (1979).
[32]P. E. Wigen, Thin Solid Films **114**, 135 (1984).
[33]A. Maksymowicz, Phys. Rev. B **33**, 6045 (1986).
[34]Z. Frait and D. Fraitová, in *Frontiers in Magnetism of Reduced Dimension Systems*, edited by P. Wigen, V. G. Bar'yakhtar, and N. Lesnik, NATO ASI Series 3 (Kluwer Academic, Dordrecht, 1998), Vol. 49, p. 121.
[35]J. Gómez, A. Butera, and J. A. Barnard, Phys. Rev. B **70**, 054428 (2004).
[36]G. T. Rado and J. R. Weertman, J. Phys. Chem. Solids **11**, 315 (1959).
[37]I. G. Cullis and M. Heath, J. Phys. F **10**, 309 (1980).
[38]*Ultrathin Magnetic Structures I*, edited by J. A. C. Bland, and B. Heinrich (Springer, Berlin, 2005), p. 79.
[39]B. Heinrich, K. B. Urquhart, A. S. Arrott, J. F. Cochran, K. Myrtle, and S. T. Purcell, Phys. Rev. Lett. **59**, 1756 (1987).
[40]L. J. Maksymowicz and H. Jankowski, J. Magn. Magn. Mater. **109**, 341 (1992).
[41]L. J. Maksymowicz, D. Sendorek-Temple, and R. Zuberek, J. Magn. Magn. Mater. **67**, 9 (1987).
[42]For FeBSi/Pd multilayers (Ref. 40) $\partial_n M_s$ is in the range 20–70 emu/cm^3/nm; for GdCoMo amorphous (Ref. 41) films $\partial_n M_s$ varies between 6 and 18 emu/cm^3/nm, and in the case of Co-SiO_2 granular films (Ref. 35) $\partial_n M_s$ is in the range 10–60 emu/cm^3/nm.
[43]S. Chikazumi, *Physics of Magnetism* (Krieger, Malabar, FL, 1978), p. 167.
[44]K.-H. Na, J.-G. Na, H.-J. Kim, P.-W. Jang, and S.-R. Lee, IEEE Trans. Magn. **37**, 1302 (2001); L. Han, U. Wiedwald, B. Kuerbanjiang, and P. Ziemann, Nanotechnology **20**, 285706 (2009).
[45]J. Spałek and A. Z. Maksymowicz, Solid State Commun. **15**, 559 (1974).
[46]J. A. Aboaf, T. R. McGuire, S. R. Herd, and E. Klokholm, IEEE Trans. Magn. **20**, 1642 (1984).
[47]T. Ichitsubo and K. Tanaka, J. Appl. Phys. **96**, 6220 (2004).
[48]D. Sander, A. Enders, and J. Kirschner, J. Magn. Magn. Mater. **200**, 439 (1999).